Commun Nonlinear Sci Numer Simulat 62 (2018) 134–145

Contents lists available at ScienceDirect

Commun Nonlinear Sci Numer Simulat

journal homepage: www.elsevier.com/locate/cnsns

Research paper

Statistical analysis of symbolic dynamics in weakly coupled chaotic oscillators

A.N. Pisarchik[a,b,*], G. Huerta-Cuellar[c], C.W. Kulp[d]

[a] Center for Biomedical Technology, Technical University of Madrid, Campus Montegancedo, Pozuelo de Alarcon, Madrid, 28223, Spain
[b] Yuri Gagarin State Technical University of Saratov, Saratov, Politehnicheskaya, 77, 410054, Russia
[c] Laboratory of Dynamical Systems, Centro Universitario de los Lagos, Universidad de Guadalajara, Enrique Díaz de León 1144, Paseos de la Montaña, Lagos de Moreno, Jalisco, 47460, Mexico
[d] Department of Astronomy and Physics, Lycoming College, Williamsport, Pennsylvania 17701, USA

ARTICLE INFO

Article history:
Received 23 June 2017
Revised 17 February 2018
Accepted 19 February 2018
Available online 21 February 2018

Keywords:
Coupled oscillators
Chaos
Phase synchronization
Stochastic analysis

ABSTRACT

The difference between phases of weakly coupled chaotic oscillators fluctuates around its average value similar to a random walk. For a very weak coupling strength, the phase difference has the same stochastic properties as a Brownian motion characterized by a -2 scaling exponent in its power spectrum, and for stronger coupling it behaves as a pink noise with a close to -1 power law. Ordinary methods of stochastic analysis based on the Fourier spectrum and detrended fluctuation analysis are not able to distinguish determinism from the time series of this phase drift. Nevertheless, determinism can be revealed by the method of ordinal pattern symbolization which allows finding forbidden patterns in the time series. The efficiency of this approach is proven with the Brownian motion, where non-occurring patterns are also detected. The robustness of the method to noise is demonstrated with coupled Rössler oscillators. The stochastic properties of phase fluctuations can be promising for cryptography and secure communication using chaotic systems.

© 2018 Published by Elsevier B.V.

1. Introduction

Chaos and noise are two important forms of dynamical movement in nature; both are irregular and unpredictable in the distant future (relative to the horizon time of the chaotic system). Because of a number of common properties, the discrimination between chaos and noise is a challenging task. Since the discovery of chaos, scientists have been faced with the problem of how to distinguish a deterministic motion from a stochastic process in natural time series [1–7]. Traditional methods are based on nonlinear forecasting by comparing predicted and actual trajectories and measuring errors [1]. The forecast accuracy diminishes with increasing time intervals for chaotic time series, which does not occur for uncorrelated noise. Another method proposed by Kaplan and Glass [2,3] suggests that all tangents to a phase space trajectory generated by a deterministic system have similar orientation independently of the position in the phase space, while stochastic time series display a phase-space dependent behavior of their tangents.

Among other approaches to distinguish between chaotic and stochastic time series are methods based on the calculation of correlation dimension and entropy. In particular, Grassberger and Procaccia [8] showed that a finite value of the corre-

* Corresponding author at: Center for Biomedical Technology, Technical University of Madrid, Campus Montegancedo, Pozuelo de Alarcon, Madrid, 28223, Spain

E-mail address: alexander.pisarchik@ctb.upm.es (A.N. Pisarchik).

https://doi.org/10.1016/j.cnsns.2018.02.025
1007-5704/© 2018 Published by Elsevier B.V.

lation dimension is a signature of deterministic dynamics. However later, Osborne and Provenzale [9] found that not all systems obey this rule; in particular, stochastic systems with power-law spectra can have finite correlation dimension. Alternatively, an entropic analysis at different resolution scales can help in the classification of chaotic or deterministic behavior of a signal. This can be done by examining the dependence of the entropy and the finite size Lyapunov exponent on the resolution [4,10]. Rosso and co-workers [5,11] proposed to combine statistical complexity and normalized Shannon entropy for construction of a causality entropy-complexity plane. In a similar way, by combining two information quantifiers, namely, the normalized Shannon entropy and the Fisher information, a causality Shannon–Fisher plane can be created, where chaotic and stochastic behaviors occupy different areas [6,12]. All these methods based on information theory significantly improve the understanding of associated time series' origins.

The problem of the distinction between chaos and noise is not easy because some deterministic systems exhibit properties of stochastic motion. A famous example is "microscopic" chaos discovered by Gaspard et al. [13]. From an entropic analysis of the experimental data on the position of a Brownian particle in a liquid, they claimed that its diffusive behavior is the consequence of chaos on the molecular scale. However later, Cencini et al. [4] showed that this result does not give direct evidence that the system is deterministic (chaotic). Furthermore, they assumed that the distinction between chaos and noise makes sense only in very peculiar cases, e.g. low-dimensional systems. Otherwise, we may only describe the system complexity using nonlinear and statistical characteristics without any definitive classification of its dynamics.

In this paper we consider a particular case of deterministic motion, the phase difference between weakly coupled chaotic oscillators near the onset of phase synchronization. The choice of this specific motion is not accidental. In this synchronous state, the phases of the coupled oscillators synchronize while the amplitudes remain uncorrelated [14]. Phase synchronization frequently occurs in weakly interacting chaotic systems, including electronic circuits [15], lasers [16], ecological systems [17], neurons [18], cardio–respiratory rhythm [19], and brain [20]. Phase synchronization is particularly relevant for biomedical applications. For example, phase synchronization and desynchronization in the brain neural network may reveal the connectivity between different brain areas, that can play a putative role in pathologies, such as schizophrenia [21], Parkinson's disease [22,23], Alzheimer's disease [24], and epilepsy [25,26], as well as in important brain functions, such as perception [27] and attention [28,29]. The existence of intrinsic noise makes the synchronization problem more complicated [30]. Therefore, the analysis of the relation between phases of coupled oscillators and the knowledge of their characteristic properties may have important practical applications in many fields of science and industry.

While instantaneous phase ϕ of a dynamical system $\dot{\mathbf{x}} = \mathbf{f}(\mathbf{x})$ in the case of an asymptotically stable limit cycle can be defined from the condition $\dot{\phi}(\mathbf{x}(t) = \text{const}$ [31], its definition for chaotic and stochastic systems is somewhat problematic. The most popular approaches to associate an instantaneous phase to a chaotic trajectory are the introduction of geometric phases, the use of the Poincaré section, Hilbert transform, and the definition of phase coordinates [14,32]. Since in our work we focus on the data analysis to distinguish determinism in time series, we have to estimate phase coordinates directly from time series of one variable only. Evidently, the geometrical definition in this case is not possible because the phase space structure is unknown. Moreover, unlike periodic systems, in stochastic and chaotic systems the phase is a function of time [32,33]. Therefore, here we use the phase definition based on the descretization of scalar time series by repetitive characteristic marker events [32,34] (such as local maxima or peaks), often observed in biomedical data, population and climate dynamics. These marker events can be associated with a phase increase of 2π, and all values of the instantaneous phase between successive maxima can be computed by linear interpolation as

$$\phi_k(t) = 2\pi k + 2\pi \frac{t - t_k}{t_{k+1} - t_k} \qquad (t_k < t < t_{k+1}), \tag{1}$$

where t_k is the time at which the kth event occurs. This phase definition is very useful for practical applications when only one system variable is available for measurement, because it allows one to obtain estimation simply from the scalar chaotic time series, computing the t_k from the times of successive local maxima or minima, without having to reconstruct a higher-dimensional phase space to explicitly find a Poincaré section.

In the regime of phase synchronization of two unidirectionally coupled chaotic oscillators, the average time difference between successive events (peaks) of the response (r) system variable $\langle \Delta t^r \rangle = \langle t^r_{k+1} - t^r_k \rangle$ is the same as that of the drive (d) system variable $\langle \Delta t^d \rangle = \langle t^d_{k+1} - t^d_k \rangle$, and both time differences are equal to the average oscillation period, i.e., $\langle \Delta t^r \rangle = \langle \Delta t^d \rangle = 1/f$ (f being the dominant frequency in the power spectrum of time series). Therefore, the phase difference between the kth peaks in time series of two coupled oscillators can be calculated as [33]

$$\delta\phi_k = \phi^r_k(t) - \phi^d_k(t) = 2\pi\,(t^r_k - t^d_k)\,f, \tag{2}$$

where $\phi^r_k(t)$ and $\phi^d_k(t)$ are the phases of the kth peak of the response and drive systems, calculated by Eq. 1.

It should be noted that the amplitude and phase dynamics of coupled chaotic oscillators are quite different, although both are deterministic. The determinism in the amplitude dynamics can easily be distinguished by different methods, e.g., by a spectral or a phase-space analysis. Specifically, the power spectrum of amplitude fluctuation $\delta x = x^r - x^d$ has a dominant frequency f close to the natural frequency f_0 of the chaotic oscillator, while the phase drift $\delta\phi(t)$ between coupled oscillators does not have any dominant frequency and manifests itself as random fluctuation. A significant difference between the amplitude and phase dynamics can be seen in phase space, where any patterns can be a signature of determinism, whereas a homogeneous structure means randomness. To illustrate this difference, we reconstruct the phase spaces for the amplitude and phase differences in two unidirectionally coupled identical chaotic Rössler oscillators (the complete system of equations

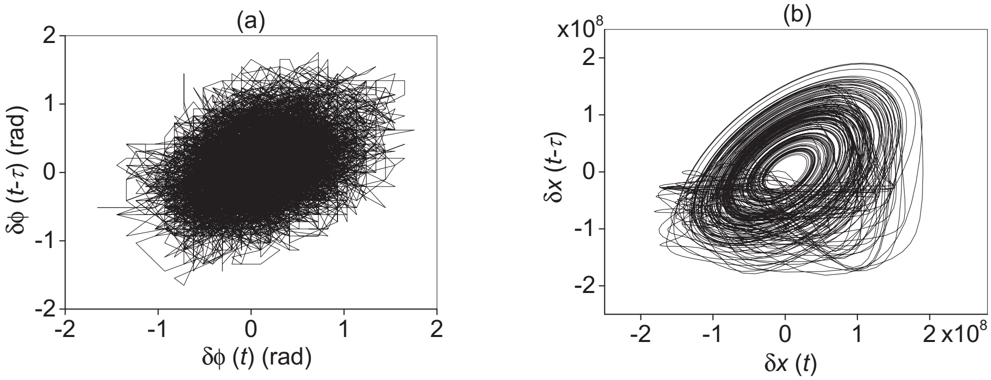

Fig. 1. Reconstructed phase spaces of the differences between (a) phases and (b) amplitudes of two coupled Rössler oscillators in the regime of phase synchronization ($\sigma = 0.005,\ \tau = 10$). The system equations and parameters are given in Sec. IV.

are presented in Sec. IV). Since we suppose that only one variable is available for measurement (say, variable x) and the complete phase space is unknown, we can only reconstruct it. For this purpose, we use the method of delayed coordinates based on the Takens Embedding Theorem [35]. The reconstructed phase spaces of the amplitude and phase fluctuations near the onset of phase synchronization are shown in Fig. 1.

One can see that while the reconstructed phase space of the amplitude difference exhibits characteristic structure, the phase difference drifts like a random walk. This means that the phase dynamics has much better stochastic properties than the amplitude dynamics. The stochastic properties of the phase fluctuation can be promising for chaotic cryptography [36] and secure communication using chaotic systems [37,38].

The analysis of the probability distribution of the first return time of the phase of a chaotic oscillator suggested that fluctuations of the chaotic phases of the intrinsic rotations about these uniform rotations behave as a fractional Brownian random process [39]. The similarity of the phase difference fluctuation to Brownian motion was also noted in coupled chaotic oscillators [34]; however, stochastic properties of this deterministic motion were not investigated, nor was its their dependence on the coupling strength.

In this paper we are interested in the following questions: What are stochastic properties of the phase difference between coupled chaotic oscillators? and How do they depend on the coupling strength? In order to answer these questions, we analyze time series generated by coupled chaotic oscillators in the vicinity of phase synchronization using modern methods of statistical and nonlinear analyses, to reveal particular scaling relations for phase dynamics. If the phase difference fluctuation exhibits stochastic properties, another important question arises: Is it possible to distinguish determinism in this motion from time series?

To identify the type of the behavior, we analyze the time series of the phase difference using three different techniques. These are a method based on the scaling law of the Fourier spectrum [40], the detrended fluctuation analysis (DFA) [41], and the detection of forbidden ordinal patterns [42]. We show that the first two methods do not allow one to distinguish determinism in the phase drift and propose an approach based on the detection of forbidden ordinal patterns in the time series, that can do it. First, we test the last method with deterministic Brownian motion and apply it to the system of coupled chaotic oscillators. Apart from its fundamental interest, this problem is of crucial importance for the analysis of experimental data when the underlying mechanism of experimentally observed fluctuations is unknown, especially in the presence of intrinsic noise inevitable in real systems.

The detection of determinism in time series data is important not only for understanding the data origin, but also for building predictive models of the system. In his book, Abarbanel [43] describes different methods of nonlinear analysis of chaotic time series. He emphasizes that standard tools of stochastic analysis, such as Fourier analysis, do not allow one to distinguish determinism in time series. To characterize chaotic motion, he proposes the methods of nonlinear analysis, such as phase-space reconstruction, fractal dimension, Lyapunov exponents, etc. However, even these methods do not guarantee that we reveal determinism in phase fluctuations. In our paper, we show that only the method of forbidden patterns with large embedding dimension can help in this situation, but it requires very long time series.

The rest of the paper is organized as follows. In Sec. II we explain how recurring and forbidden patterns can be identified in time series and used to detect determinism. In Sec. III we calculate forbidden ordinal patterns in stochastic and deterministic Brownian motions to detect determinism. Then, in Sec. IV we consider the model of coupled Rössler oscillators and apply Fourier analysis, detrended fluctuation analysis, and the method for the detection of forbidden ordinal patterns. We also study the robustness of the last method to noise. Finally, the main conclusions are given in Sec. V.

2. Identifying determinism in time series data

Discriminating between deterministic and stochastic dynamics is an important problem in time series analysis. Tests for determinism can be very helpful when trying to distinguish deterministic chaotic behavior from stochastic dynamics.

One such test developed by Kaplan and Glass [2] which uses an embedding of the time series, and tracks the so-called image of a point. In deterministic systems, nearby points will have nearby images. Other tests involve fitting models to time series [44], the use of permutation slopes [45], and looking for repeated patterns in symbol spectra [46], just to name a few. The method used here will focus on finding so-called *forbidden patterns* in the time series. The method is fast, easy to interpret, and easy to implement on a large number of series. Furthermore, it benefits from the advantages of the Bandt-Pompe (BP) methodology of symbolization [47], as discussed below.

Identifying patterns in a time series can be difficult because there can be a large number of different values in the series. In order to establish patterns, a time series needs to symbolized. In other words, the elements of the time series need to be replaced by a limited number of symbols, called an *alphabet*. The simplest symbolization is a threshold-based binary symbolization where a threshold value is chosen and elements greater (less) than the threshold are reassigned the value 1 (0). Time series elements equal to the threshold can be assigned either 0 or 1. It can be difficult [48] to choose a value of the threshold such that the resulting binary series captures all of the dynamics of the original series.

To avoid some of those difficulties, Bandt and Pompe [47] developed a dynamics difference-based symbolization method that avoids using a threshold and is robust to noise. Furthermore, symbol distribution resulting from the BP methodology is invariant with respect to nonlinear monotonous transformations and copes well with nonstationarities. The BP methodology groups elements of the time series together in a fashion similar to phase space reconstruction methods. The method is as follows. The time series $\{x_1, x_2, \ldots, x_n\}$ is partitioned into embedding vectors $\{x_i, x_{i+\tau}, \ldots x_{i+(d-1)\tau}\}$, where, similar to phase space reconstruction, d and τ are called *embedding dimension* and *embedding delay*, respectively. Each d-dimensional vector is mapped to a permutation of the set $\{1, 2, \ldots, d\}$ based on the ranking of each element in the vector. The permutations are called *ordinal patterns*. For example, the vector {8, 7, 15, 12} can be mapped to the ordinal pattern {2, 1, 4, 3} because $x_2 < x_1 < x_4 < x_3$. In the case of two or more equal elements, elements are sorted by their index such that {11, 13, 11, 15} maps to the ordinal pattern {1, 3, 2, 4}. For simplicity, each ordinal pattern can be labeled with an integer called an *ordinal pattern index*. The exact mapping from ordinal pattern to ordinal pattern doesn't matter as long as the mapping is consistent. For example, we could map the ordinal pattern {1, 2, 34} to the ordinal pattern index, 1. Likewise, we could map {2, 1, 4, 3} to the ordinal pattern index 8. The resulting symbolized series would then consist of a list of ordinal pattern indices with an alphabet length of $d!$.

As opposed to choosing a threshold, the BP methodology requires a choice of two parameters, τ and d. There is no prescribed method of choosing τ. For example, similar to creating embedding vectors for phase space reconstruction, τ can be chosen to be the first zero of the autocorrelation function or the first local minimum of the mutual information. In addition, τ can be chosen to match a time scale of interest in the time series. In this paper, we follow the work done in [46] and choose $\tau = 1$, which was used there to successfully identify stochasticity in series which produced false positives in other tests for determinism. The choice of d will be discussed later.

The BP methodology can be used to detect deterministic dynamics in a time series. As mentioned previously, deterministic series will have certain ordinal patterns that occur often and other ordinal patterns that do not occur at all. The latter patterns are called *forbidden patterns* and correspond to states inaccessible to the deterministic system. Stochastic time series, on the other hand, will not have forbidden patterns because all states are accessible if measurements are made for a long enough period of time. Since the time series of a deterministic system has forbidden patterns [42,49], the number of forbidden patterns (NFP) can be used as a measure of the system determinism.

In order to identify recurring and forbidden patterns in time series, the *permutation spectrum test* (PST) can be used [46]. The PST is capable of detecting determinism in correlated random systems which are incorrectly identified as deterministic by other tests. Furthermore, the PST can recognize determinism in systems which have been falsely identified as stochastic by other tests. In this paper, we use a modified version of the PST which focuses only on the identification of forbidden patterns in the series. The measure of only the NFP can be useful in cases where one is analyzing multiple time series and working with permutation spectra can be cumbersome. The identification of forbidden patterns is done by symbolizing the entire series into ordinal patterns and counting how many of the $d!$ ordinal patterns do not appear in the time series.

In order to identify forbidden patterns in a series of length, N, the embedding dimension, d, must be carefully chosen such that $d! \ll N$. If too large a value of d is chosen, then there simply may not be enough data to sample all possible $d!$ ordinal patterns in the series. The patterns not detected in the series may only be missing and not forbidden. Hence, if d is too large for the series, then a stochastic series may be falsely identified as deterministic.

In this paper, the value of d is chosen using the following method. An ensemble of pseudo random time series is produced with a length, N, the same length of the series for which we are interested in detecting determinism. Each series of the pseudo random ensemble is then symbolized using the Bandt–Pompe methodology for a given value of d. The number of missing patterns (NMP), ordinal patterns not appearing in the series, is computed for each series in the ensemble. The value of d chosen for analysis is the largest d that produces a zero NMP for all elements of the ensemble, providing us evidence that the patterns missing from the series are forbidden and are not missing due to small sample effects. Following this methodology, we will refer to the ordinal patterns not appearing a series as forbidden and not missing. Of course, a value of d such that most, but not all, of the series in the ensemble produce NMP $= 0$ could be chosen, In such a case, the percentage of series with NMP $= 0$ could serve as a confidence interval for the analysis. In this paper, we will use time series long enough such that any patterns missing from the series are most likely forbidden and therefore will equate missing patterns with forbidden ones.

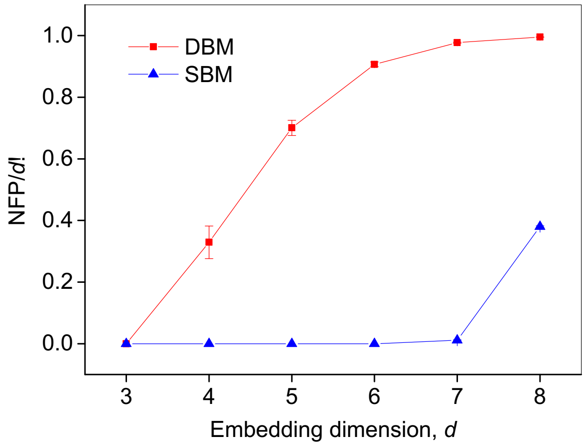

Fig. 2. Percentage of forbidden patterns (NFP) as a function of embedding dimension for DBM (red squares) and SBM (blue triangles) systems. (For interpretation of the references to colour in this figure legend, the reader is referred to the web version of this article.)

The choice of using the largest value of d producing NFP $= 0$ for all members of the ensemble is made with the hope that d is large enough to capture the dynamics of the series. Just as choosing too large a value of d can lead to small sample effects and a false positive for determinism, it has been the authors' experience that choosing too small of a value for d can lead to a false rejection of determinism in the data. In other words, one may obtain NFP $= 0$ for small values of d. This is believed to be due to the embedding dimension being too small to accurately capture the dynamics, similar to using too small of a dimension in phase space reconstruction.

The random series in the ensemble can be generated using a probability distribution function similar to that of the series of interest. For example, in the next section, the systems of interest are known to behave similar to Wiener processes, and hence, Wiener processes with mean zero and unit variance are used to produce the random ensemble. For systems with unknown underlying dynamics, surrogate series which preserve various properties (one of the most common being the power spectrum) of the original series can be generated [50] for the ensemble.

In the next sections, we will apply the method of forbidden ordinal patterns first to both the stochastic and deterministic Brownian motions and then to the phase difference between two coupled chaotic Rössler oscillators.

3. Analysis of stochastic and deterministic Brownian motions

In order to demonstrate the ability of the BP approach to effectively detect determinism in time series, we compute the number of forbidden ordinal patterns (NFP) for deterministic and stochastic Brownian motions. The deterministic Brownian motion (DBM) was generated using the approach proposed in Ref [7]., where the DBM generator based on the Langevin equation with additional degree of freedom was proposed as follows

$$\begin{aligned} \dot{x} &= y, \\ \dot{y} &= -\gamma y + z, \\ \dot{z} &= -\alpha_1 x - \alpha_2 y - \alpha_3 z + \alpha_4, \end{aligned} \tag{3}$$

where x, y, z are variables and $\alpha_{1,\,2,\,3}$ are constants. The first two equations are derived from the Langevin equation [51] with a little change: the stochastic term is replaced by the deterministic term z. The third equation in Eq. (3) is the rate of a change in acceleration known as *jerk* [52] derived in the same spirit as those introduced by Campos-Cantón et al. [53]. Finally, α_4 is defined as

$$\alpha_4 = C_1 * \mathrm{Round}(x/C_2), \tag{4}$$

where $C_1 = 0.9$ and $C_2 = 0.6$ are constants which determine the system equilibrium and the function Round(K) rounds K to a nearest integer less than or equal to K.

The time series analysis showed that DBM exhibited typical characteristics of stochastic Brownian motion (SBM), namely, a linear growth of the mean square displacement and an approximately -2 power law of the frequency spectrum [13]. Furthermore, an approximately 3/2 power law scaling of the fluctuation function versus segmented lengths was obtained by DFA [41], and confirmed a Brownian character of the observed motion. Thus, the previous results showed that the main characteristics of DBM did not represent a subtle difference from traditional SBM.

Here, we are interested in whether or not the BP methodology can distinguish determinism in DBM. Fig. 2 shows the results of finding the number of forbidden patterns (NFP) as a function of embedding dimension d for multiple time series generated from SBM and DBM systems. The vertical axis of Fig. 2 is scaled by dividing NFP by $d!$, the maximum number of possible ordinal patterns when an embedding dimension of d is used. As was mentioned previously, NFP $= 0$ means that there are no forbidden patterns in the series, i.e. the series is stochastic, whereas a nonzero NFP implies the presence of determinism.

Fig. 2 was produced using two ensembles of data, one generated from a SBM system and the other from the DBM system. The SBM series were generated using *Mathematica*'s Wiener Process command. Each ensemble consists of 50 series that are 131 072 elements long. Each series in each ensemble was symbolized using the BP methodology for a given value of d and the NFP for each series was found. The ensemble mean and standard deviation of the NFP was then calculated. In many cases, the error bars in Fig. 2 are smaller than the plot markers representing the mean.

The first result obtained from Fig. 2 is that for $d=3$, the DBM ensemble produces NFP = 0. This is an example of the aforementioned false rejection of determinism when too small of an embedding dimension is used. Notice that as d increases, the number of forbidden patterns for $d \geq 4$ increases. At first glance, it would appear that determinism can be detected in the DBM system using a value of d as large as 8. However, inspection of the SBM results shows that it is not the case and illustrates the second result. The second result of Fig. 2 displays small sample effects for our systems. For the SBM system, the equality NFP = 0 fulfills for $d \leq 6$. Although it is difficult to see due to the scale of Fig. 2, the mean NFP/d! is 0.04 for $d=7$, i.e. there are approximately an average of 201 forbidden patterns in each SBM series when $d=7$. The nonzero value of the NFP in the SBM ensemble implies that 131 072 elements are not enough to reliably detect stochasticity in the system 100% of the time. When analyzing the DBM system with the same length using $d \geq 7$, we need to keep in mind that there is a low chance of falsely detecting determinism. The possibility of a false detection of determinism in these series increases 10 times with $d=8$, as the NFP/d! for the SBM in the case of $d=8$ is approximately 0.4. Hence, at least some of the patterns in the DBM series identified as forbidden in our analysis are, in fact, missing due to small sample effects when $d \geq 7$ is used. Notice that for $d=7$ and $d=8$ it appears that the NFP/d! for the DBM system approaches one, but is not equal to one. For these two embedding dimensions there are very few patterns that occur in series compared to the number of possible patterns (which is large).

The actual value of the NFP for the DBM system in Fig. 1 for $4 \leq d \leq 6$ is not necessarily important. The analysis of time series generated from discrete maps has shown that periodic systems tend to have more forbidden patterns than chaotic series [46]. However, in continuous systems this does not necessarily hold true because the number of forbidden patterns depends on the sampling time for the series [54]. Hence, although tempting, one should not identify high values of NFP as a stronger measure of determinism than lower values of NFP. A purely deterministic system with a few forbidden patterns can have the same NFP value as a system with a large NFP value, but also has noise. That said, for a given system, the NFP of the series should decrease as noise levels increase. Thus, the presence of forbidden patterns is enough to identify determinism.

4. Phase fluctuation in coupled chaotic Rössler oscillators

To generate the time series of the phase difference between coupled chaotic oscillators, we use the model of two unidirectionally coupled Rössler oscillators given as

$$\begin{aligned}
\dot{x}_m &= -y_m - z_m, \\
\dot{y}_m &= x_m + a y_m, \\
\dot{z}_m &= b + z_m(x_m - c), \\
\\
\dot{x}_s &= -y_s - z_s, \\
\dot{y}_s &= x_s + a y_s + \sigma(y_m - y_s), \\
\dot{z}_s &= b + z_s(x_s - c),
\end{aligned} \tag{5}$$

where the subindices m and s refer to the drive (master) and response (slave) oscillators, respectively, and σ is the coupling strength varied between 10^{-4} and 10^{-2} with a step of 10^{-4}. The parameters $a=0.165$, $b=0.2$, and $c=10$ used in this work provide chaotic oscillations.

The numerical simulations of Eq. (5) are carried out using the fourth-order Runge–Kutta algorithm of MATLAB with a 0.1 integration step size. In this paper, we analyze the time series of 5.5×10^5 data points. We compare the time series of the drive and response oscillators and calculate the phase difference by Eq. (2). The time series of $\delta\phi$ for two different values of the coupling strength are shown in Figs. 3(a) and 3(c). The difference between these two time series is notable. While for a very weak coupling $\delta\phi$ gradually increases in time (Fig. 3(a)), for a stronger coupling the phase difference fluctuates, during a relatively long time, around zero within the range from $-\pi$ to π radians, and then suddenly switches to 2π rad (Fig. 3(c)). Such a well-known phase flip behavior occurs very rarely when the system is close to the transition point to phase synchronization [55].

The phase drift in Figs. 3(a) and 3(c) can be characterized by the mean square displacement (MSD), i.e., the deviation over the whole time series duration T, between the phase difference $\delta\phi$ and its time-averaged value $\langle\delta\phi\rangle_T$, defined as

$$\mathrm{MSD}(t) = \left\langle [\delta\phi(t) - \langle\delta\phi\rangle_T]^2 \right\rangle, \tag{6}$$

One can see from Fig. 3(d) that MSD displays a linear dependence in time, $\mathrm{MSD} = 2Dt$, which is the typical feature of the Brownian motion, where D is the diffusion coefficient. This result, first obtained by Einstein, is related to Stokes' law [56,57].

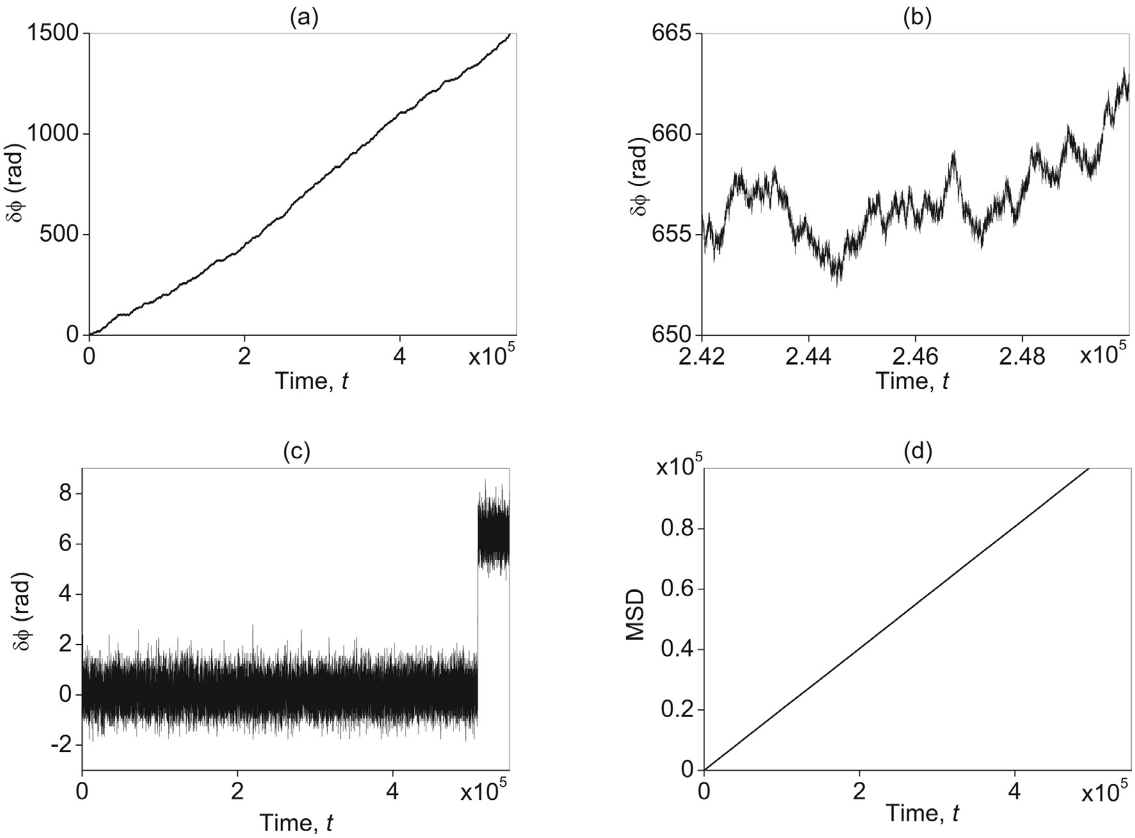

Fig. 3. Time series of (a-c) phase difference between two coupled chaotic Rössler oscillators Eq. 1 for coupling (a,b) $\sigma = 0.001$ and (c) $\sigma = 0.005$, and (d) MSD calculated by Eq. (2) for $\sigma = 0.005$ and $T = 551590$. The time series in (b) is an enlarged part of that in (a).

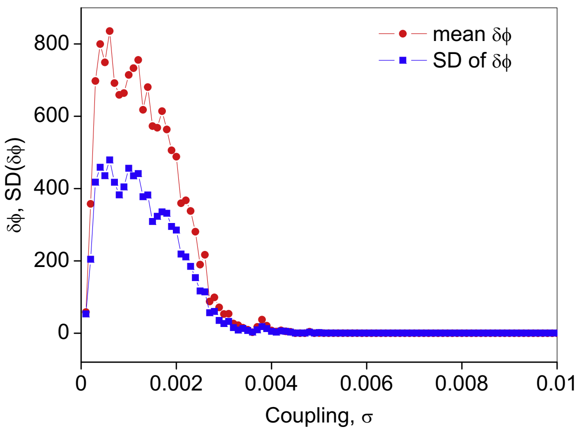

Fig. 4. Mean phase difference $\langle\delta\phi\rangle$ (dots) and standard deviation of phase difference SD($\delta\phi$) (squares) as a function of coupling.

The diffusion analysis is out of the scope of this paper (for interested readers we recommend Refs [58–60].). For sufficiently long time series, the average phase difference $\langle\delta\phi\rangle_T$ does not depend on T, and therefore MSD is only a function of time t.

Phase synchronization can also be characterized by the mean phase difference $\langle\delta\phi\rangle$ and the standard deviation of the phase difference SD($\delta\phi$) from the mean [14]. Fig. 4 shows how these values depend on the coupling strength. One can clearly distinguish two different regions in these dependencies. In the first region, for very weak coupling ($\sigma < 0.004$), both $\langle\delta\phi\rangle$ and SD($\delta\phi$) depend on the coupling and reach maxima at $\sigma \approx 0.001$ as σ is increased, whereas in the second region, for stronger coupling ($\sigma > 0.004$) they are close to zero and independent of the coupling.

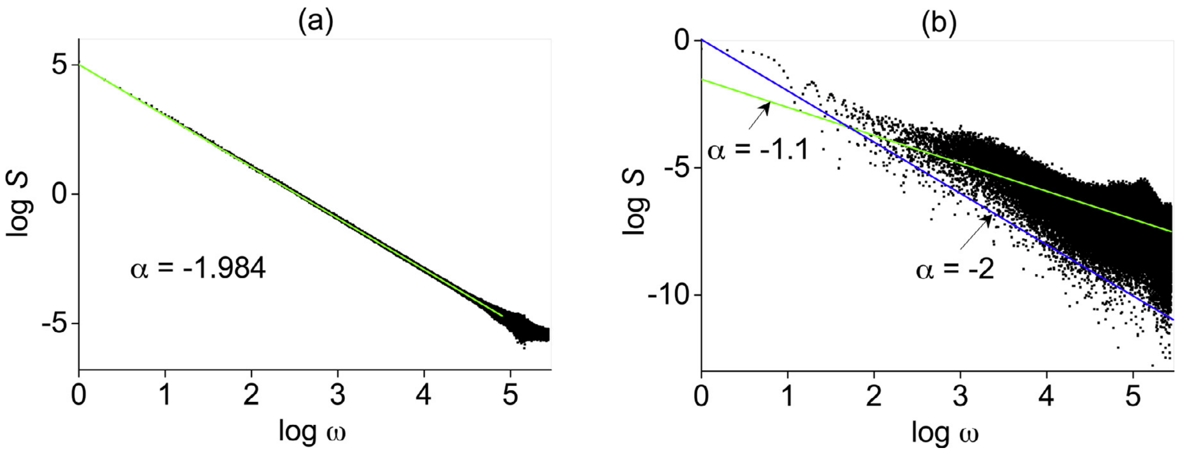

Fig. 5. Power spectra of phase difference $\delta\phi$ for (a) $\sigma = 0.001$ and (b) $\sigma = 0.005$, exhibiting $\alpha = -1.984 \pm 0.001$ and $\alpha = -1.100 \pm 0.003$ power laws (green lines), typical for a Brownian motion and pink noise, respectively. The blue line in (b) shows the -2 slope for reference. (For interpretation of the references to colour in this figure legend, the reader is referred to the web version of this article.)

4.1. Fourier analysis

In order to better understand the dynamics of the phase drift, we take the Fourier transform of the $\delta\phi$ time series and analyze the power spectrum $S(\omega)$

$$S(\omega) \sim \omega^{\alpha}, \tag{7}$$

on a log-log scale by linear approximation for searching scaling exponent α.

The power spectra of the phase drift $\delta\phi$ for two different values of the coupling strengths, $\sigma = 0.001$ and (b) $\sigma = 0.005$, are shown respectively in Figs. 5(a) and (b). These spectra are approximated by linear dependencies with scaling exponents $\alpha \approx -2$ and $\alpha \approx -1$ obtained by the least squares method. The -2 scaling exponent is typical for the Brownian motion found in the experiments of Gaspard et al. [13] with colloidal particles. In our case, this scaling fits the spectrum very well for very small coupling ($0.0001 < \sigma < 0.0023$), whereas for a little stronger coupling ($0.0023 < \sigma < 0.01$) the phase drift is approximated by the -1 scaling exponent, typical for pink noise. In Fig. 5(b) we also plot for reference a -2 slope (blue line). One can see that the -1 slope is more convincing in the high frequency range, while for low frequencies the slope is closer to -2.

4.2. Detrended fluctuation analysis (DFA)

Stochastic properties of a system can be revealed by analyzing its self-affinity, i.e. self-similarity of fractal objects obtained by their rescaling in the x- and y-directions using an anisotropic affine transformation [61]. The statistical self-affinity can be determined using the method of *detrended fluctuation analysis* (DFA) [62] which allows quantitative characterization of long-time correlation of non-stationary signals.

The DFA method works as follows. The bounded time series $\delta\phi(t)$ of T samples is first integrated or summarized into an unbounded process $\Phi(k)$ known as *cumulative sum* or *profile*:

$$\Phi(k) = \sum_{t=1}^{k} \left[\delta\phi(t) - \langle \delta\phi(t) \rangle \right], \tag{8}$$

where $\langle \delta\phi(t) \rangle$ is the average phase difference over time T. This integration process converts the phase drift into a random walk, i.e. maps the original time series to a self-similar process. To measure the vertical characteristic scale of the integrated time series we divide $\Phi(k)$ into $N = T/n$ time windows Φ_n of equal length n and in each window we fit the data by a least squares straight line which represents the local *trend* of the window. The y coordinate of the trends is denoted as $\Phi_n(k)$. For a given window size n, the characteristic size of fluctuation for this integrated and detrended time series is calculated as

$$F(n) = \left(\frac{1}{T} \sum_{k=1}^{T} \left[\left(\Phi(k) - \Phi_n(k) \right)^2 \right] \right)^2. \tag{9}$$

This computation is repeated over all time scales to provide a relationship between $F(n)$ and the box size n. A linear dependence in the log-log graph indicates the presence of scaling (self-similarity), i.e., the fluctuations in small boxes are related to the fluctuations in larger boxes as the power law

$$F(n) \sim n^{\beta}. \tag{10}$$

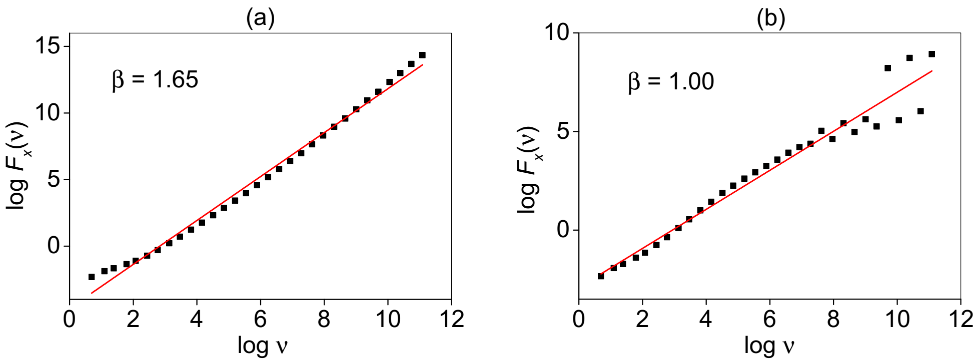

Fig. 6. Characteristic size of the phase difference fluctuation versus the box size for coupling (a) $\sigma = 0.001$ and (b) $\sigma = 0.005$. The straight lines represent linear fits with scaling exponents 1.65 ± 0.05 and 1.00 ± 0.04, typical for a Brownian motion and pink noise, respectively.

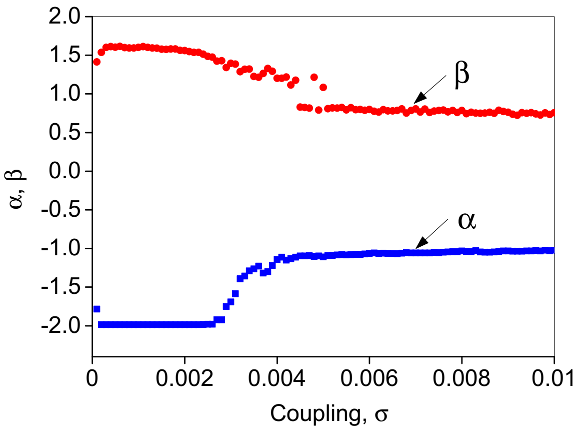

Fig. 7. Scaling exponents α (blue squares) and β (red dots) versus coupling strength. (For interpretation of the references to colour in this figure legend, the reader is referred to the web version of this article.)

The scaling exponent β (self-similarity parameter) is calculated as the slope of a straight line fit to the log-log graph of $F(n)$ against n using least-squares. This exponent is a generalization of the Hurst exponent. When the exponent is about or larger than 1, three different random behaviors can be distinguished.

For $\beta \sim 1$, DFA defines $1/f$ or pink noise.
For $\beta > 1$, DFA defines a non-stationary unbounded behavior.
For $\beta \sim 3/2$, DFA defines a Brownian motion.

Fig. 6 displays the results of the DFA analysis of the time series shown in Fig. 3(c,d). One can see that for weak coupling the phase drift behaves as a Brownian motion with the scaling exponent close to 3/2, whereas for stronger coupling the phase difference has a pink noise property with $\beta = 1$.

Both the Fourier analysis and DFA show that the phase difference of weakly coupled chaotic oscillators behaves as a Brownian motion. This can be seen from Fig. 7, where we plot the scaling exponents α and β versus the coupling strength. These exponents are obtained by two different methods, spectral density $I(\omega)$ and DFA, respectively. Indeed, for very small coupling ($\sigma < 2.3 \times 10^{-3}$) the phase drift has the properties of Brownian motion with $\alpha \approx -2$ and $\beta \approx 3/2$. However, for stronger coupling, the type of the behavior is different. When σ is increased, α increases and β decreases, approaching $\alpha \approx -1$ and $\beta \approx 1$, so that the behavior becomes more correlated. For $\beta \approx 1$, the DFA defines $1/f$ or pink noise.

4.3. Method of forbidden patterns

In this section we apply the method of forbidden patterns to the time series analyzed above in order to see if determinism can be detected. In addition, we test the BP method for its robustness to noise. In other words, do forbidden patterns persist in the series even when noise is present? If so, how much noise is needed to have zero missing patterns, i.e., all possible ordinal patterns appear in the series?

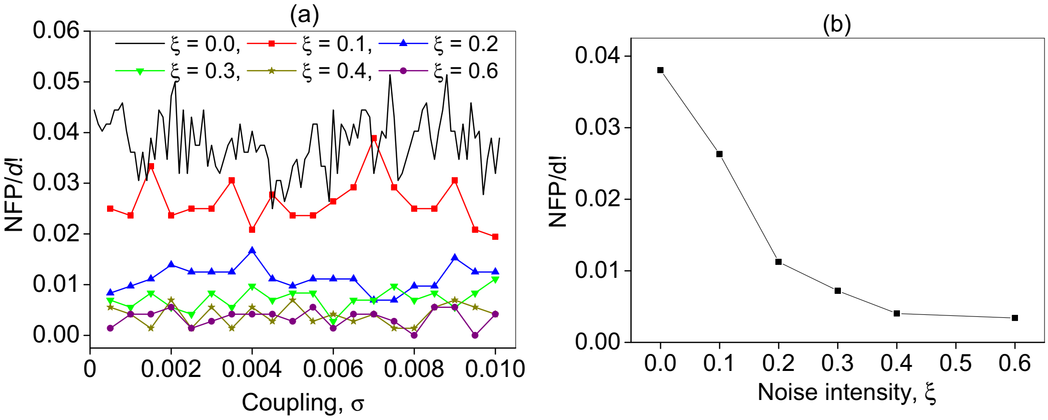

Fig. 8. Number of forbidden patterns (NFP/d!) in phase difference between coupled chaotic Rössler oscillators as a function of (a) coupling strength and (b) noise intensity, for $d = 6$.

In order to study the robustness of the BP method to noise, we add noise to both the drive and the response Rössler oscillators, as follows

$$\begin{aligned}
\dot{x}_m &= -y_m - z_m, \\
\dot{y}_m &= x_m + a y_m + \xi_m w_m, \\
\dot{z}_m &= b + z_m (x_m - c), \\
\\
\dot{x}_s &= -y_s - z_s, \\
\dot{y}_s &= x_s + a y_s + \sigma (y_m - y_s) + \xi_s w_s, \\
\dot{z}_s &= b + z_s (x_s - c).
\end{aligned} \tag{11}$$

Here, w_m and w_s are a pair of independent normally distributed random variables with zero expectation and 0.1 variance (equal to the integration step), generated using the Box-Müller transform as

$$\begin{aligned}
w_m &= \sqrt{-2\log(u_1)\cos(2\pi u_2)}, \\
w_s &= \sqrt{-2\log(u_2)\sin(2\pi u_1)},
\end{aligned} \tag{12}$$

where u_1 and u_2 are a pair of independent random numbers uniformly distributed in the interval (0, 1), and ξ_m and ξ_s are the noise intensities. The Box-Müller transformation is one of the most popular methods for generating pseudo-random samples from a normal distribution [63]. The detailed explanation of this method can be found in Ref [64]. For simplicity, we suppose that the drive and response oscillators are subject to noise with the same intensity, i.e., $\xi_m = \xi_s = \xi \in [0, 1]$. In our calculations, we use the Matlab code published in Ref [65]. The noise is applied at each Runge-Kutta integration step.

In Fig. 8(a) we plot the number of forbidden patterns found in the time series of the phase difference for different coupling strengths between the Rössler oscillators Eq. (11) in the absence (upper trace) and in the presence of noise with different intensities (lower traces). We study fewer couplings for the noisy cases because of the computational expense involved in generating the noisy series. As seen in Fig. 8(a), the NFP appears to be independent of coupling strength for $0 \le \sigma < 0.01$. However, as the noise increases, we see that the NFP generally decreases, as expected. The value of NFP/d!, averaged over the range of coupling strengths from 0 to 0.01, is plotted in Fig. 8(b) as a function of the noise intensity ξ. Eventually, as ξ exceeds 0.4, almost zero forbidden patterns are found, again demonstrating that at these coupling strengths and noise levels, the NFP tends to decrease with noise level. Here, we use the embedding dimension $d = 6$. To test if there are enough data points in each time series to reliably use this value of d, an ensemble of 1000 pseudo-random series, each with a length of 140 000 elements, is created from a uniform distribution, and the NFP of each series is computed. We found that all of the uniform random time series have zero number of forbidden patterns (NFP = 0). In addition, we performed a similar test using a fractional Gaussian noise (fGn) process with a Hurst exponent of $H = 0.9$, in order to see if 140 000 elements are enough to detect randomness in a highly correlated time series. Of the 1000 fGn series tested, all of them had NFP = 0. Hence, we can be confident in the detection of determinism in the Rössler system even in the presence of relatively strong noise.

5. Conclusion

Using ordinary methods of stochastic analysis, we have characterized the phase difference between coupled chaotic oscillators in the vicinity of phase synchronization. Our results indicate that the phase drift exhibits stochastic properties which depend of the coupling strength. While near the onset of phase synchronization the phase difference behaves as a Brownian motion with the scaling exponent in its power spectrum close to -2, for stronger coupling the phase difference obeys a -1 power law, typical for pink noise. The traditional methods of stochastic analysis, such as Fourier and detrended fluctuation analyses, were not able to distinguish determinism in the time series of the phase difference for a very weak coupling. Only the detection of forbidden ordinal patterns using the Bandt–Pompe methodology revealed determinism in the phase fluctuations. The forbidden patterns test has also been applied to find the difference between stochastic and deterministic Brownian behaviors. Due to its robustness to noise, the method of forbidden patterns can be used for the analysis of experimental data to reveal determinism in noisy time series.

To distinguish determinism in phase fluctuations, a large embedding dimension ($d \geq 7$) should be used, that requires very long time series. This property is very promising for designing a pseudo random number generator to be used in chaotic cryptography and secure communication, where information can be encoded with relatively short time series.

Although in this work we explored a classical example of coupled chaotic Rössler oscillators frequently used for studying phase synchronization, we believe that similar results can be obtained in other systems. The significant contribution of our paper is that the identification of missing patterns in the series is able to detect determinism for phase fluctuations, when other methods fail to do so.

Acknowledgments

A. N. P. acknowledges support from the Ministry of Economy and Competitiveness (Spain) (project SAF2016-80240). C. W. K. acknowledges support from Lycoming College. The model development has been supported by the Russian Science Foundation (grant 17-72-30003).

References

[1] Sugihara G, May RM. Nonlinear forecasting as a way of distinguishing chaos from measurement error in time series. Nature 1983;344:734–41. doi:10.1038/344734a0.
[2] Kaplan DT, Glass L. Direct test for determinism in a time series. Phys Rev Lett 1992;68:427–30. doi:10.1103/PhysRevLett.68.427.
[3] Kaplan DT, Glass L. Coarse-grained embeddings of time series: random walks. Gaussian random processes, and deterministic chaos, Physica D 1993;64:431–54. 0167-2789/93
[4] Cencini M, Falcioni M, Olbrich E, Kantz H, Vulpiani A. Chaos or noise: difficulties of a distinction. Phys Rev E 2000;62:427–37. doi:10.1103/PhysRevE.62.427.
[5] Rosso OA, Larrondo HA, Martín MT, Plastino A, Fuentes MA. Distinguishing noise from chaos. Phys Rev Lett 2007;99:154102. doi:10.1103/PhysRevLett.99.154102.
[6] Olivares F, Plastino A, Rosso OA. Contrasting chaos with noise via local versus global information quantifiers. Phys Lett A 2012;376:1577–83. doi:10.1016/j.physleta.2012.03.039.
[7] Huerta-Cuellar G, Jiménez-López E, Campos-Cantón E, Pisarchik AN. An approach to generate deterministic brownian motion. Commun Nonlinear Sci Numer Simulat 2014;19:2740–6. doi:10.1016/j.cnsns.2014.01.010.
[8] Grassberger P, Procaccia I. Characterization of strange attractors. Phys Rev Lett 1983;50:346–9. doi:10.1103/PhysRevLett.50.346.
[9] Osborne AR, Provenzale A. Finite correlation dimension for stochastic systems with power-law spectra. Physica D 1989;35:357–81. doi:10.1016/0167-2789(89)90075-4.
[10] Kantz H, Olbrich E. Coarse grained dynamical entropies: investigation of high-entropic dynamical systems. Physica A 2000;280:34–48. doi:10.1016/S0378-4371(99)00616-0.
[11] Rosso OA, et al. Causality and the entropycomplexity plane: robustness and missing ordinal patterns. Physica A 2012;391:42–55. doi:10.1016/j.physa.2011.07.030.
[12] Olivares F, Plastino A, Rosso OA. Ambiguities in bandt-pompe's methodology for local entropic quantifiers. Physica A 2012;391:2518–26. doi:10.1016/j.physa.2011.12.033.
[13] Gaspard P, et al. Experimental evidence for microscopic chaos. Nature 1998;394:865–8. doi:10.1038/29721.
[14] Pikovsky A, Rosenblum M, Kurths J. Synchronization: A Universal concept in nonlinear science. New York: Cambridge Univ. Press; 2001.
[15] Parlitz U, Kocarev L, Stojanovski T, Preckel H. Encoding messages using chaotic synchronization. Phys Rev E 1996;53:4351–61. doi:10.1103/PhysRevE.53.4351.
[16] Pisarchik AN. Recent achievements in laser dynamics: control and synchronization. Kerala: Research Singpost; 2008.
[17] Blasius B, Huppert A, Stone L. Complex dynamics and phase synchronization in spatially extended ecological systems. Nature 1999;399:354–9. doi:10.1038/20676.
[18] Makarenko V, Llinás R. Experimentally determined chaotic phase synchronization in a neuronal system. Proc Natl Acad Sci USA 1998;95:15747–52. doi:10.1073/pnas.95.26.15747.
[19] Schäfer C, Rosenblum MG, Kurths J, Abel HH. Heartbeat synchronized with ventilation. Nature 1998;392:239–40. doi:10.1038/32567.
[20] Bhattacharya J, Petsche H. Enhanced phase synchrony in the electroencephalograph γ band for musicians while listening to music. Phys Rev E 2001;64:012902. doi:10.1103/PhysRevE.64.012902.
[21] Lynall ME, Bassett DS, Kerwin R, McKenna PJ, Kitzbichler M, Muller U, Bullmore E. Functional connectivity and brain networks in schizophrenia. J Neuroscience 2010;30:9477–87. doi:10.1523/JNEUROSCI.0333-10.2010.
[22] Tass PA, Fieseler T, Dammers J, Dolan K, Morosan P, Majtanik M, Boers F, Muren A, Zilles K, Fink GR. Synchronization tomography: a method for three-dimensional localization of phase synchronized neuronal populations in the human brain using magnetoencephalography. Phys Rev Lett 2003;90:088101. doi:10.1103/PhysRevLett.90.088101.
[23] Dubbelink KTO, Hillebrand A, Stoffers D, Deijen JB, Twisk JW, Stam CJ, Berendse HW. Disrupted brain network topology in parkinson's disease: a longitudinal magnetoencephalography study. Brain 2014;137:197–207. doi:10.1093/brain/awt316.
[24] Stam CJ, et al. Graph theoretical analysis of magnetoencephalographic functional connectivity in alzheimer's disease. Brain 2009;132:213–24. doi:10.1093/brain/awn262.
[25] Takeshita D, Bahar S. Synchronization analysis of voltage-sensitive dye imaging during focal seizures in the rat neocortex. Chaos 2011;21:047506. doi:10.1063/1.3640043.
[26] Moskalenko OI, Koloskova AD, Zhuravlev MO, Koronovskii AA, Hramov AE. Intermittent phase synchronization in human epileptic brain. Proc SPIE 2017;10063:1006316. doi:10.1117/12.2249950.
[27] Rodriguez E, George N, Lachaux JP, Martinerie J, Renault B, Varela FJ. Perception'S shadow: longdistance synchronization of human brain activity. Nature 1999;397:430–3. doi:10.1038/17120.

[28] Roy A, Steinmetz PN, Hsiao SS, Johnson KO, Niebur E. Synchrony: a neural correlate of somatosensory attention. J Neurophysiol 2007;98:1645–61. doi:10.1152/jn.00522.2006.

[29] Fries P, Reynolds JH, Rorie AE, Desimone R. Modulation of oscillatory neuronal synchronization by selective visual attention. Science 2001;291:1560–3. doi:10.1126/science.291.5508.1560.

[30] Deco G, Jirsa VK, McIntosh AR, Sporns O, Kötter R. Key role of coupling, delay, and noise in resting brain fluctuations. Proc Natl Acad Sci USA 2009;106:10302–7. doi:10.1073/pnas.0901831106.

[31] Park Y, Heitmann S, Ermentrout GB. The utility of phase models in studying neural synchronization. 2017. ArXiv: 1707.05713.

[32] Freund JA, Schimansky-Geier L, Hänggi P. Frequency and phase synchronization in stochastic systems. Chaos 2003;13:225–38. doi:10.1063/1.1500497.

[33] Boccaletti S, Pisarchik AN, del Genio CI, Amann A. Synchronization: from coupled systems to complex networks. Cambridge University Press; 2018. ISBN: 9781107056268

[34] Pisarchik AN, Jaimes-Reátegui R, Villalobos-Salazar JR, Garcia-Lopez JH, Boccaletti S. Synchronization of chaotic systems with coexisting attractors. Phys Rev Lett 2006;96:244102. doi:10.1103/PhysRevLett.96.24410.

[35] Takens F. Detecting strange attractors in turbulence. Lecture Notes in Mathematics, Volume 898. Berlin: Springer-Verlag; 1981. ISBN 978-3-540-11171-9

[36] Baptista MS. Cryptography with chaos. Phys Lett A 1998;240:50–4. doi:10.1016/S0375-9601(98)00086-3.

[37] García-López JH, Jaimes-Reategui R, Chiu-Zarate R, Lopez-Mancilla D, Jimenez RR, Pisarchik AN. Secure computer communication based on chaotic rössler oscillators. The Open Electrical and Electronic Engineering Journal 2008;2:41–4. doi:10.2174/1874129000802010041.

[38] Jiménez-Rodríguez M, Jaimes-Reátegui R, Pisarchik AN. Secure communication based on chaotic cipher and chaos synchronization. Discontinuity, Nonlinearity and Complexity 2012;1:57–68. doi:10.5890/DNC.2012.02.003.

[39] Yalçinkaya T, Lai YC. Phase characterization of chaos. Phys Rev Lett 1997;79:3885–8. doi:10.1103/PhysRevLett.79.3885.

[40] Handel PH, Chung AL. Noise in physical systems and 1/f fluctuations. New York: American Institute of Physics; 1993.

[41] Peng CK, Buldyrev SV, Havlin S, Simons M, Stanley HE, Goldberger AL. Mosaic organization of DNA nucleotides. Phys Rev E 1994;49:1685–9. doi:10.1103/PhysRevE.49.1685.

[42] Amigó JM, Zambrano S, Sanjuán MAF. True and false forbidden patterns in deterministic and random dynamics. Europhys Lett 2007;79:50001. doi:10.1209/0295-5075/79/50001.

[43] Abarbanel HDI. Analysis of observed chaotic data. New York: Springer; 1995. ISBN 978-1-4612-0763-4

[44] Chon KH, Kanters JK, Cohen RJ, Holstein-Rathlou NH. Detection of chaotic determinism in time series from randomly forced maps. Physica D 1997;99:471–86. doi:10.1016/S0167-2789(96)00159-5.

[45] Fouda JSAE, Koepf W. Detecting regular dynamics from time series using permutations slopes. Commun Nonlinear Sci Numer Simulat 2015;27:216–27. doi:10.1016/j.cnsns.2015.03.008.

[46] Kulp CW, Zunino L. Discriminating chaotic and stochastic dynamics through the permutation spectrum tes. Chaos 2014;24:033116. doi:10.1063/1.4891179.

[47] Bandt C, Pompe B. Permutation entropy: a natural complexity measure for time series. Phys Rev Lett 2002;88:174102. doi:10.1103/PhysRevLett.88.174102.

[48] Bollt EM, Stanford T, Lai YC, Ẑyczkowski K. Validity of threshold-crossing analysis of symbolic dynamics from chaotic time series. Phys Rev Lett 2000;85:3524–7. doi:10.1103/PhysRevLett.85.3524.

[49] Amigó JM, Zambrano S, Sanjuán MAF. Detecting determinism in time series with ordinal patterns: a comparative study. Int J of Bifurcation and Chaos 2010;20:2915–24. doi:10.1142/S0218127410027453.

[50] Schreiber T, Schmitz A. Surrogate time series. Physica D 2000;142:346–82. doi:10.1016/S0167-2789(00)00043-9.

[51] Langevin P. On the theory of brownian motion. C R Acad Sci Paris 1908;146:530–3.

[52] Sprott JC. Some simple chaotic jerk functions. Am J Phys 1997;65:537–43. doi:10.1119/1.18585.

[53] Campos-Cantón E, Barajas-Ramirez JG, Solis-Perales G, Femat R. Multiscroll attractors by switching systems. Chaos 2010;20:013116. doi:10.1063/1.3314278.

[54] Kulp CW, Chobot JM, Niskala BJ, Needhammer CJ. Using forbidden ordinal patterns to detect determinism in irregularly sampled time series. Chaos 2016;26:023107. doi:10.1063/1.4941674.

[55] Osipov GV, Hu B, Zhou C, Ivanchenko MV, Kurths J. Three types of transitions to phase synchronization in coupled chaotic oscillators. Phys Rev Lett 2003;91:024101. doi:10.1103/PhysRevLett.91.024101.

[56] Einstein A. On the movement of small particles suspended in a stationary liquid demanded by the molecular kinetic theory of heat. Ann Phys 1905;17:549–60.

[57] Einstein A. On the theory of the brownian movement. Ann Phys 1906;19:371–81.

[58] Stratonovich RL. Topics in the theory of random noise, volume 2. CRC Press, First Edition; 1967. ISBN-10: 0677007906

[59] Neiman A, Schimansky-Geier L, Cornell-Bell A, Moss F. Noise-enhanced phase synchronization in excitable media. Phys Rev Lett 1999;83:4896–9. doi:10.1103/PhysRevLett.83.4896.

[60] Amro RM, Lindner B, Neiman AB. Phase diffusion in unequally noisy coupled oscillators. Phys Rev Lett 2015;115:034101. doi:10.1103/PhysRevLett.115.034101.

[61] Mandelbrot BB. Self-affine fractals and fractal dimension. Phys Scr 1985;32:257–60. http://stacks.iop.org/1402-4896/32/i=4/a=001

[62] Peng CK, Havlin S, Stanley HE, Goldberger AL. Quantification of scaling exponents and crossover phenomena in nonstationary heartbeat time series. Chaos 1995;5:82–7. doi:10.1063/1.166141.

[63] Box GEP, Müller ME. A note on the generation of random normal deviates. Ann Math Statist 1958;29:610–11. 1958

[64] Press WH, Teukolsky SA, Vetterling WT, Flannery BP. Numerical recipes: the art of scientific computing, third edition. Cambridge University Press; 2007.

[65] Zahri M. Colored-noise-like multiple ito-stochastic integrals: algorithms and numerics. Journal of Numerical Mathematics and Stochastics 2015;7:73–95.